Quantization of hyperspectral image manifold using probabilistic distances

Gianni FRANCHI, Jesús ANGULO

CMM-Centre de Morphologie Mathématique,
MINES ParisTech, PSL-Research University

GSI 2015 2nd conference on Geometric Science of Information
October 2015

Plan

Hyperspectral images

Hyperspectral image consists of a simultaneous acquisition of spectrum of reflected light at each pixel of the image.

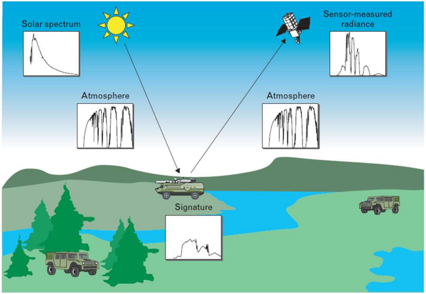

Figure: Taking of an ultra/hyper-spectral image by a satellite [1]

[1] Manolakis, D., Marden, D., & Shaw, G. A. (2003). Hyperspectral image processing for automatic target detection applications. Lincoln Laboratory Journal, 14(1), 79-116.

Hyperspectral images

There are two ways to manipulate Hyperspectral images:

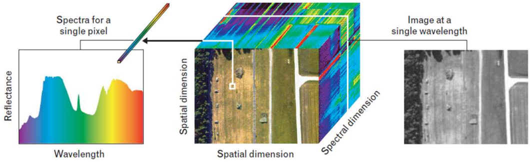

Figure: Representation of an hyperspectral image[2]

- Disadvantage: this type of image contains redundant information: correlated variables
- High dimensionality : Hyperspectral images = hundred of channels / ultraspectral picture = thousand of channels

[2] Manolakis, D., Marden, D., & Shaw, G. A. (2003). Hyperspectral image processing for automatic target detection applications. Lincoln Laboratory Journal, 14(1), 79-116.

State of the art on hyperspectral data distances

- Chang, C. I. (2003). Hyperspectral imaging: techniques for spectral detection and classification (Vol. 1). Springer Science & Business Media.
- Paclik, P., & Duin, R. P. (2003). Dissimilarity-based classification of spectra: computational issues. Real-Time Imaging, 9(4), 237-244.
- Ma, L., Crawford, M. M., & Tian, J. (2010). Local manifold learning-based-nearest-neighbor for hyperspectral image classification. Geoscience and Remote Sensing, IEEE Transactions on, 48(11), 4099-4109.
- Crawford, M. M., Ma, L., & Kim, W. (2011). Exploring nonlinear manifold learning for classification of hyperspectral data. In Optical Remote Sensing (pp. 207-234). Springer Berlin Heidelberg.
- Gueguen, L., Velasco-Forero, S., & Soille, P. (2014). Local mutual information for dissimilarity-based image segmentation. Journal of mathematical imaging and vision, 48(3), 625-644.

Model of the data

Let us denote by

- $n \in \mathbb{N}$ the number of pixel on the image. So the number of spectra;
- $X = (x_1, \dots, x_d) \in \mathbb{R}^d$, and $Y = (y_1, \dots, y_d) \in \mathbb{R}^d$, two different spectra of the image;

It is possible to normalize them, such that they have the same norm 1, let us consider $P_x = (\frac{x_1}{\sum_i x_i}, \dots, \frac{x_d}{\sum_i xi}) \in \mathbb{R}^d$ and $P_y = (\frac{y_1}{\sum_i y_i}, \dots, \frac{y_d}{\sum_i y_i}) \in \mathbb{R}^d$, which represent the normalize version of these vectors.

Model of the data

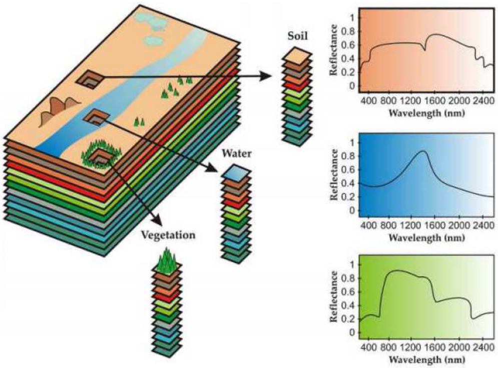

Figure: Representation of an hyperspectral image[3]

[3] ALTMANN, Y., DOBIGEON, N., MACLAUGHLIN, S., & TOURNERET, J. Y. Démélange non-linéaire d'images hyperspectrales à l'aide de fonctions radiales de base et de moindres carrés orthogonaux.

Model of the data

- Let us denote by $R \in \mathbb{N}$ the number of class on the image, which is link with the number of materials.
- Let us consider that we have a ground truth.

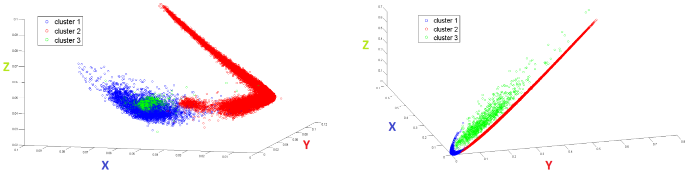

(a) (b)

Figure: Scatter plot of distances of pixels (of Pavia image) of cluster 1 (in blue) to the centroid of cluster 1 in X, to to the centroid of cluster 2 in Y, to the centroid of cluster 3 in Z. Similarly, in red for cluster 2, and in green for cluster 3. In (a) we use the L_2 norm as dissimilarity measure, in (b) we used the Kullback-Leibler divergence.

Goal

- First, we want to find a distance that would separate data from different clusters, without any prior knowledge.
- Then our goal would be to quantize the hyperspectral image according to these distance, and to spatial information.

L_p Minkowski norms on pdf and SAM and spherical distance

We used the $p-$norm.

$$\|P_x - P_y\|_p = \left(\sum_i |P_{x,i} - P_{y,i}|^p\right)^{\frac{1}{p}}$$

.

We can consider that each pixel X follow a multinomial distribution of parameter P_x. It is then possible to define a Fisher-Rao distance between X, Y, represented by their pdf P_x, P_y, which is the spherical distance:

$$D_{Spher}(X, Y) = 2\arccos(\sum \sqrt{P_{x,i} P_{y,i}})$$

Their are some similarities with a distance that is classically used on hyperspectral images:the SAM, which can be defined between X, Y as :

$$D_{SAM}(X, Y) = \arccos(\frac{\sum X_i Y_i}{\sqrt{\sum X_i X_i}\sqrt{\sum Y_i Y_i}}) = \frac{1}{2} D_{Spherical}(X^2, Y^2)$$

This metric is invariant to spectral multiplication since $D_{SAM}(\alpha X, Y) = D_{SAM}(X, Y)$, $\forall \alpha \in \mathbb{R}^*$. So it is invariant to illumination changes, which can be problematic on remote sensing.

Rényi divergences

We can use on hyperspectral image divergence, that are called the Rényi divergence of order α, $\alpha > 0$ of a distribution P_x from a distribution P_y:

$$S_\alpha(P_x \| P_y) = \frac{1}{\alpha - 1} \log \sum_i P_{x,i}^{\alpha} P_{y,i}^{1-\alpha}.$$

$S_{\alpha \to 1}(P_x \| P_y) = S(P_x \| P_y)$ where S is the kullback divergence defined by :

$$S(P_x \| P_y) = \sum_i P_{x,i} \log \frac{P_{x,i}}{P_{y,i}}$$

if $\alpha = 1/2$ we have $S_{\alpha=1/2}(P_x \| P_y) = -2 \log \left(1 - D_{Hellinger}(X,Y)/2\right)$; where $D_{Hellinger}$ is the Hellinger distance defined by :

$$D_{Helli}(X,Y) = (1/\sqrt{2}) \left(\sum_{i=1}^{d} (\sqrt{P_{x,i}} - \sqrt{P_{y,i}})^2 \right)^{1/2},$$

and the case $\alpha = 2$ leads to the quadratic Rényi divergence, which is $S_{\alpha=2}(P_x \| P_y) = \log \left(1 + D_{\chi^2}(X,Y)\right)$, where D_{χ^2} is the χ^2 distance defined by :

$$D_{\chi^2}(X,Y) = \sum_{i=1}^{d} \frac{\left(P_{x,i} - m_i\right)^2}{m_i}$$

$$\text{with } m_i = \frac{P_{x,i} + P_{y,i}}{2},$$

Mahalanobis distance

We can consider a classical model on hyperspectral image which assumes that each spectrum X follows is corrupted by an additive multivariate normal noise of mean 0 and with a fixed covariance for all the spectra. So if we write X the real spectra and Y the observation we that $Y = X + N$ and so $Y \sim \mathcal{N}(\mu_Y, \Sigma)$, with $\mu_Y = X$. It turns out that the Fisher-Rao distance between Z, Y happens to be the Mahalanobis distance defined by:

$$D_{\text{Mahalanobis}}(Z, Y) = (\mu_Z - \mu_Y)^T \Sigma^{-1} (\mu_Z - \mu_Y) \quad (1)$$

Then there is the question on how to assess Σ.

Earth Mover distance

Let us consider two spectra X and Y, represented by their respective pdf P_x, P_y. Their Earth Mover Distance can be defined by:

$$D_{\text{EMD}}(P_x, P_y) = \min_{\alpha_{i,j} \in \mathcal{M}} \left(\sum_{i=1}^{d} \sum_{j=1}^{d} \alpha_{i,j} C(i,j) \right)$$

where $\mathcal{M} = \{\alpha_{i,j} \geq 0; \sum_{i=1}^{d} \alpha_{i,j} = P_{y,j}; \sum_{j=1}^{d} \alpha_{i,j} == P_{x,i}\}$ and C is the cost function. Different choices of cost functions have been considered. Here we will choose two different cost functions. The first one can be defined as:

$$C_1(i,j) = \frac{1}{d} |i - j|$$

In this case, it happens that the Earth Mover Distance is:

$$D_{\text{EMD1}}(P_x, P_y) = \frac{1}{d} \|C_x - C_y\|_1$$

the other cost function selected is :

$$C_2(i,j) = \begin{cases} |i-j| \text{ if } |i-j| \leq s \\ s \text{ otherwise} \end{cases}$$

where s is the value of the threshold. We will write this distance D_{EMD2}.

Quantization

Quantization is the process which allows to approach a signal with large set of values by a signal on a smaller set. Images are signals on a spatial domain, so their quantization should takes into account the expected spatial coherence. To achieve this goal, we choose to use $\alpha-$connected components representation [4] [5], that produces an image partition into homogenous spatial classes.

---

[4]Soille, P. (2008). Constrained connectivity for hierarchical image partitioning and simplification. Pattern Analysis and Machine Intelligence, IEEE Transactions on, 30(7), 1132-1145.

[5]Gueguen, L., Velasco-Forero, S., & Soille, P. (2014). Local mutual information for dissimilarity-based image segmentation. Journal of mathematical imaging and vision, 48(3), 625-644.

Quantization

Given a distance $d : \mathbb{R}^d \times \mathbb{R}^d \longrightarrow \mathbb{R}$, two pixels $(f(x), f(y)) \in (\mathbb{R}^D)^2$ belong to the same $\alpha-$connected components of f if and only if there is a path $(p_0, \ldots, p_n) \in E^n$ such as $p_0 = x$ and $p_n = y$ and if $\forall i \in [1, n-1]$, $d(f(p_i), f(p_{i+1})) \leq \alpha$ and $\alpha \in \mathbb{R}^+$

Figure: Quasi-flat zone of the pavia hyperspectral image, there are 84931 clusters.

Quantization

- First a partition of an image to work with superpixels;
- then we transform the image representation into a graph representation called the region adjacency graph (RAG). It is a graph where each node is a superpixel, and edges represent the dissimilarity between superpixels.

(a)

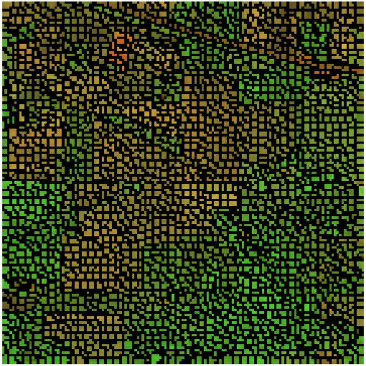

(b)

Quantization

We represent each node (which is a set of pixels) of the graph by the barycentre according to the metric of the set of pixels P, which is defined by :

$$m = \arg\min_{m \in P} \sum_{x_i \in P} d(m, x_i). \tag{2}$$

If all the weights are equal, we say simply that m is the geometric median. Then we calculate the $\alpha-$connected components of the graph.

Results

To evaluate the measures we used different criteria.

		Predicted class		
		$\mathcal{C}_1$	$\mathcal{C}_2$	$\mathcal{C}_3$
Actual class	$\mathcal{C}_1$	C_{11}	C_{12}	C_{13}
	$\mathcal{C}_2$	C_{21}	C_{22}	C_{23}
	$\mathcal{C}_3$	C_{31}	C_{32}	C_{33}

The Overall accuracy:

$$OA = \frac{\sum_{i=1}^{3} C_{ii}}{\sum_{i=1}^{3}\sum_{j=1}^{3} C_{ij}} \times 100 \tag{3}$$

The Class Accuracy of class i:

$$CA_i = \frac{C_{ii}}{\sum_{j=1}^{3} C_{ij}} \times 100 \tag{4}$$

The Class Accuracy of class i:

$$AA = \frac{\sum_{i=1}^{3} CA_i}{3} \times 100 \tag{5}$$

Results

Results on "Pavia" image										
	L_1	L_2	L_∞	D_{Spher}	D_{SAM}	D_{Helli}	D_{χ^2}	S	$S_{\alpha=1/2}$	$S_{\alpha=2}$
OA	0.001	0.001	0.003	0.012	0.056	0.001	0.23	0.51	0.50	0.50
AA	0.001	0.001	0.013	0.085	0.12	0.001	0.11	0.25	0.22	0.22
Rank	0.93	0.93	0.91	0.81	0.62	0.46	0.33	0.21	0.47	0.22
SNR	22.82	22.96	22.89	22.72	14.90	21.92	23.90	21.88	21.97	21.20

Results on "Pavia" image						
	SID	D_{Mahal1}	D_{Mahal2}	D_{Kolmo}	D_{EMD1}	D_{EMD2}
OA	0.012	0.009	0.057	0.006	0.008	0.006
AA	0.089	0.003	0.22	0.09	0.1	0.08
Rank	0.36	0.58	0.37	0.90	0.90	0.41
SNR	21.26		21.4	22.0	22.47	

Table: Comparison of probabilistic distances on hyperspectral images.

Results

Results on "Indian Pines" image										
	L_1	L_2	L_∞	D_{Spher}	D_{SAM}	D_{Helli}	D_{χ^2}	S	$S_{\alpha=1/2}$	$S_{\alpha=2}$
OA	0.016	0.016	0.011	0.016	0.09	0.016	0.30	0.010	0.010	0.010
AA	0.012	0.0022	0.014	0.016	0.13	0.016	0.24	0.09	0.09	0.09
Rank	0.44	0.45	0.45	0.45	0.22	0.46	0.18	0.46	0.44	0.45
SNR	12.86	12.74	12.73	12.73	5.59	12.69	14.01	12.88	12.81	12.86

Results on "Indian Pines" image						
	SID	D_{Mahal1}	D_{Mahal2}	D_{Kolmo}	D_{EMD1}	D_{EMD2}
OA	0.010	0.019	0.068	0.0162	0.029	0.0162
AA	0.09	0.016	0.13	0.0019	0.069	0.016
Rank	0.46	0.39	0.34	0.45	0.45	0.42
SNR	12.73		12.74	11.01	12.55	

Table: Comparison of probabilistic distances on hyperspectral images.

Results

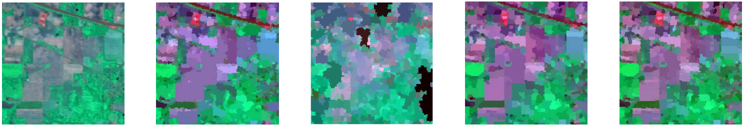

(a) (b) (c) (d) (e)

Figure: (a) False RGB color image (using three spectral bands) of Indian Pines hyperspectral image. False RGB color image of the quantized hyperspectral image thanks to in (b) the norm 2, (c) the SAM, (d) the χ^2 distance, (e) the EMD.

Results

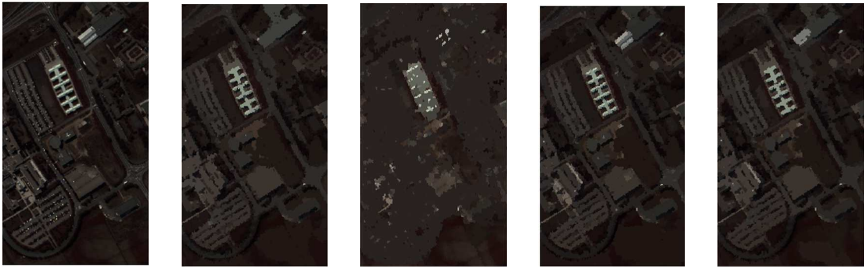

(a) (b) (c) (d) (e)

Figure: (a) False RGB color image (using three spectral bands) of Pavia hyperspectral image. False RGB color image of the quantized hyperspectral image $K = 3000$ thanks to in (b) the norm 2, (c) the SAM, (d) the χ^2 distance, (e) the EMD.